On Understanding Microemulsions

II. Thermodynamics of Droplet-Type Microemulsions

J. TH. G. OVERBEEK, G. J. VERHOECKX, P. L. DE BRUYN, AND H. N. W. LEKKERKERKER

Van't Hoff Laboratory, University of Utrecht, Padualaan 8, 3584 CH Utrecht, The Netherlands

Received July 7, 1986; accepted December 1, 1986

A thermodynamic theory of microemulsions containing brine, oil, an ionic surfactant, and a nonionic cosurfactant is given. Conditions for phase equilibria are derived. The treatment is limited to droplet-type microemulsions with emphasis on W/O + W systems. Important features are saturation adsorption of surfactant and cosurfactant, the interfacial bending stress, the standard chemical potential of the droplets in the free energy of mixing, and a quantitative treatment of the contribution of the electric double layer to the bending stress. Numerical illustrations show good agreement with experimental data on the influence of salt and cosurfactant on droplet size and interfacial tension in W/O + W equilibria.

INTRODUCTION

In the last decade many publications have appeared on the thermodynamics of microemulsions. Their main aim is to understand why these concentrated mixtures of oil and water are stable and what determines the phase equilibria in such multicomponent systems.

In the phase diagram we encounter microemulsions of spherical droplets of oil in water and of water in oil with a continuous transition between the two extreme types. In the transition region bicontinuous, not necessarily ordered, structures must be present. This can be illustrated with the familiar Winsor-type equilibria (1, 2) as sketched in Fig. 1. Furthermore ordered arrangements (lamellar, hexagonal, cubic) occur in the phase diagrams.

This paper is limited to droplet-type microemulsions and their equilibria with noncolloidal oily or aqueous phases, with emphasis on Winsor II systems (W/O) with an ionic surfactant and a nonionic cosurfactant.

Of the many authors who have been active in this field we mention Reiss (3), Ruckenstein and Chi (4), Wagner (5), Robbins (2), Overbeek *et al.* (6), Miller *et al.* (7), Mitchell and Ninham (8), Huh (9), and Safran and Turkevich (10), who all dealt mainly with droplet-type microemulsions. Talmon and Prager (11), however (see also the beautiful feature article by de Gennes and Taupin (12)), used a model primarily adapted to nondroplet-type systems and good for dealing with critical behavior in the phase equilibria.

In the theories of microemulsions the following three elements play a role: a very low or zero interfacial tension, as already suggested by Schulman (13); the free energy of mixing of the droplets with the continuous medium (e.g., the hard sphere variant as used by Vrij *et al.* (14)); and the free energy of bending of the interface of the droplets. The bending effect implies that the interfacial tension tension depends significantly on the curvature as has also been suggested by Bowcott and Schulman (13) and by Winsor (1). A more quantitative approach has been given by Robbins (2) and by Miller *et al.* (7).

The low interfacial tension is due to the adsorption of surfactant and cosurfactant (see, e.g., Overbeek (6)). Its dependence on curva-

0021-9797/87 $3.00

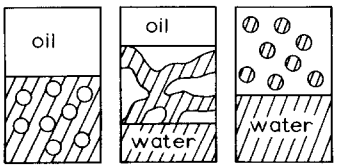

FIG. 1. Microemulsions O/W in equilibrium with oil (type I), W/O in equilibrium with water (more precisely a noncolloidal aqueous phase) (type II), and bicontinuous (O + W) in equilibrium with oil and water (type III). This sketch does not imply that the transition between droplet type and bicontinuous microemulsions coincides with the transition from two-phase to three-phase equilibria. In microemulsions composed of brine, an ionic surfactant, a nonionic cosurfactant, and a hydrocarbon oil the transition from type I via type III to type II is effected by an increase in ionic strength and/or an increase in cosurfactant concentration.

ture derives from the influence of the curvature on the free energy of the electric double layer and on the degree of crowding of the hydrophobic tails of the surfactants. Without significant influence of the bending term the competition between the interfacial tension and the free energy of mixing would either produce a very large number of very small drops (mixing prevalent) or a very high volume fraction of the droplets (low interfacial tension prevalent).

New in this paper is a more complete thermodynamic formulation with special attention to the standard chemical potential of the droplets and to the saturation adsorption of surfactant and cosurfactant. Furthermore a new treatment of the effect of the curvature of the electric double layer is given.

THERMODYNAMIC EQUATIONS

In the following theory we first formulate the Gibbs energy of a microemulsion, minimize it with respect to internal equilibrium, and then minimize the Gibbs energy of a combination of a microemulsion with an excess of the liquid in the droplets (W/O + W or O/W + O). The equilibrium conditions lead to relations for the interfacial tension and the bending stress as functions of the droplet radius and volume fraction. A model for the dependence of the bending stress on the concentrations of salt and cosurfactant then allows us to calculate the droplet radius and the interfacial tension between the macroscopic phases, which can be compared with experimental data.

The Gibbs energy, G^M, of a microemulsion can be written

$$G^M(T,p,n_i \cdots n_j \cdots) = \sum \mu_i(T,p,n_i \cdots n_j \cdots)n_i, \quad [1]$$

where n_i and μ_i are the amount and the chemical potential respectively of component i and T and p are temperature and ambient pressure respectively. Since the pressure in the droplets may differ from the pressure p, we derive G^M from the Helmholtz free energy F^M according to

$$G^M = F^M + pV^M, \quad [2]$$

where V^M is the volume of the microemulsion.

F^M is built up in two steps. In the first step we consider n_d drops in local equilibrium with the surrounding continuous medium of the microemulsion, but the drops are still fixed in the laboratory coordinates (e.g., hanging on the tip of a "submicrosyringe"). All chemical potentials, λ_i, are equal in the drops, in the continuous medium, and in the interfaces, but λ_i is not necessarily equal to μ_i. In the second step the drops are allowed to move freely in the medium, thus liberating the free energy of mixing, F_{mix}.

The components, i, are water (w); an ionic surfactant (Nasa), e.g., sodium dodecyl sulfate, SDS; a nonionic cosurfactant (co), e.g., pentanol; a salt, e.g., NaCl; and a hydrocarbon oil (o), e.g., cyclohexane. The droplets are indicated by the subscript, d, the continuous medium by the subscript, m. Volume changes upon mixing and adsorption are neglected.

The Helmholtz free energy can be written as

$$F^M = \sum n_i\lambda_i - pV_m - (p+\Delta p)V_d + \sigma A + F_{mix}, \quad [3]$$

where V_m is the volume of the continuous medium, V_d is that of the droplets, and $p + \Delta p$ is the pressure inside the droplets (i.e., at the center of the droplets, where there is no electric field; more precisely the pressure extrapolated to the value it would have far from the electric double layer). The interface is described as having no volume (just the Gibbs dividing plane). This can be reconciled with the assumption of finite molar volumes by a suitable combination of positive and negative adsorptions. σ is the interfacial tension between droplets and medium. It is essential to take σ as curvature dependent at constant T, p, and λ_i's. A is the total area of the interface.

Then G^M is obtained as

$$G^M = F^M + pV^M = \sum n_i\lambda_i - \Delta pV_d + \sigma A + G_{mix}, \quad [4]$$

where $V^M = V_m + V_d$ and $G_{mix} = F_{mix}$.

Since we have to minimize G^M in order to find the equilibrium conditions for the microemulsion, we also need dG^M:

$$dG^M = \sum n_i d\lambda_i + \sum \lambda_i dn_i - \Delta p dV_d - V_d d\Delta p + \sigma dA + Ad\sigma + dG_{mix}. \quad [5]$$

σ depends on all λ_i's, but also explicitly on the curvature which is expressed by

$$Ad\sigma = A\sum\left(\frac{\partial\sigma}{\partial\lambda_i}\right)_a d\lambda_i + A\left(\frac{\partial\sigma}{\partial(2/a)}\right)_{\lambda_i} d\left(\frac{2}{a}\right) = -A\sum\Gamma_i d\lambda_i + Acd\left(\frac{2}{a}\right), \quad [6]$$

where Γ_i is the amount of component i adsorbed per unit area and

$$c = \left[\partial\sigma/\partial\left(\frac{2}{a}\right)\right]_{T,p,\lambda_i} \quad [7]$$

is the bending stress coefficient (15–17), expressing that G^M changes at constant area, A, when the radius, a, or the curvature, $2/a$, is changed. For simplicity we assume from here on that all droplets have the same radius, a, which agrees with experimental evidence, at least for not too large drops.

The curvature influence was already recognized by Gibbs (17), who also remarked that c can be made zero by a judicious choice of the Gibbs dividing surface. In our case this is not practical since we want to focus attention on the influence of physical changes in curvature, and at low interfacial tensions, the $c = 0$ surface may be far away from the region of strong interfacial inhomogeneity.

Equation [5] can be simplified by applying Eq. [6], the Gibbs–Duhem equations, for the continuous medium and the droplets,

$$(\sum n_{i,m} d\lambda_i - V_m dp)_T = 0 \quad [8]$$

$$(\sum n_{i,d} d\lambda_i - V_d d(p + \Delta p))_T = 0, \quad [9]$$

and equations for the conservation of components,

$$n_i = n_{i,m} V + n_{i,d} + A\Gamma_i. \quad [10]$$

dG^M then becomes

$$(dG^M)_{p,T} = \sum \lambda_i dn_i - \Delta p dV_d + \sigma dA + Acd\left(\frac{2}{a}\right) + dG_{mix}. \quad [11]$$

THE FREE ENERGY OF MIXING

Vrij *et al.* (14) have demonstrated that the osmotic pressure of the droplets in certain W/O microemulsions corresponds over a wide range of concentrations with the pressure of a hard sphere fluid as given by the equations of Percus and Yevick (18) and Carnahan and Starling (19). Overbeek (6) used these equations in 1978 to derive that

$$G_{mix} = n_d kT\left(\ln\phi - 1 + \phi\frac{4 - 3\phi}{(1-\phi)^2} + \frac{\mu_d^\theta}{kT}\right), \quad [12]$$

where ϕ is the volume fraction of the droplets, seen as hard spheres, n_d is their number, and μ_d^θ is their standard chemical potential. Many authors agree in essence on the concentration-dependent part of G_{mix}, but there is no unanimity about the choice of μ_d^θ.

Robbins (2), Wagner (5), and Mitchell and Ninham (8) left the mixing term out com-

pletely. Ruckenstein and Chi (4), Overbeek (6, 1978), and Miller *et al.* (7) use

$$\mu_d^\theta = kT \ln \frac{v_1}{v_d}, \qquad [13]$$

where v_1 is the molecular volume of the continuous medium and v_d is the volume of one droplet. This corresponds to writing for μ_d at high dilution

$$\mu_d(\phi \to 0) = kT(\ln x_d - 1), \qquad [14]$$

where x_d is the mole fraction of the droplets. Safran and Turkevich (10) use $\mu_d^\theta = 0$. Huh (9) uses a rather different equation for G_{mix}, which does not contain the ln ϕ term, but starts with a term proportional to ϕ. Overbeek *et al.* (6, 1984) rejected the choice as made in Eq. [13], because in the chosen model molecular properties of the medium should not occur. They put

$$\mu_d^\theta = -18.25\, kT \qquad [15]$$

which makes $G_{mix} = 0$ for close packing ($\phi = 0.74$).

Finally the approach already used by Reiss (3) in 1975 was later also adopted by Overbeek (6, 1985). Here

$$\mu_d^\theta = -\frac{3}{2} kT \ln \frac{12n}{\pi} = -\frac{3}{2} kT \ln \frac{16a^3}{v_w}, \qquad [16]$$

where n is the number of water molecules (in a W/O microemulsion) in a droplet, a the radius of the droplets and v_w the molecular volume of water.

Reiss' work was primarily developed in connection with nucleation theory, but his 1975 paper (3) is explicitly aimed at the problem of thermodynamically stable emulsions. He argues that there is a difference in entropy between a droplet fixed in the laboratory, for which the free energy is correctly described by $1/n_d$ of the first three terms of Eq. (4), and a similar droplet subject to free Brownian displacement in the dispersion medium. The difference can be reduced to the translational freedom of the center of mass of the droplet. The center of mass of the free droplet can move through the whole volume V^M and this freedom for n_d droplets results in a term $n_d kT \times \ln(n_d/V^M)$ in G_{mix} (Eq. [12]), if the interactions among the droplets are neglected. The center of mass of the fixed drop can only move through a small fraction of the drop volume, which Reiss finds to be

$$v_d \Big/ \left(\frac{12n}{\pi}\right)^{3/2}. \qquad [17]$$

The numerical factor is model sensitive. The $(12/\pi)^{3/2}$ is valid for a spherical droplet containing n hard sphere molecules at a density equal to one-half of the close packed density. The factor $v_d/n^{3/2}$ can be understood in the following way. Each of the molecules can be displaced over a distance $\pm b$ in the x, y, and z directions. b is of the order of the radius of the droplet. If the displacements are randomly distributed over plus and minus, the average sum of the displacements in one coordinate is $|b\sqrt{n}|$. The coordinates of each molecule contribute $1/n$ to the coordinates of the center of mass. Consequently the center of mass (c.o.m.) moves around in a volume

$$V_{c.o.m.} \simeq \left(\frac{b\sqrt{n}}{n}\right)^3 = b^3 n^{-3/2} \simeq v_d n^{-3/2}. \qquad [18]$$

The relative increase in freedom of displacement of the center of mass is given by $V^M/V_{c.o.m.}$ and the factor $n_d kT \ln(n_d/V^M)$ in G_{mix} as mentioned above must be replaced by $n_d kT \times \ln(n_d V_{c.o.m.}/V^M)$ which, when we use Eq. [17], leads to

$$\begin{aligned} G_{mix} &= n_d kT \left(\ln \frac{n_d v_d}{V^M} \left(\frac{\pi}{12n}\right)^{3/2} - 1 + \phi \frac{4-3\phi}{(1-\phi)^2} \right) \\ &= n_d kT \left(\ln \phi - 1 + \phi \left(\frac{4-3\phi}{(1-\phi)^2}\right) - \frac{3}{2} \ln \frac{12n}{\pi} \right) \qquad [19] \\ &= n_d kT \left(\ln \phi - 1 + \phi \left(\frac{4-3\phi}{(1-\phi)^2}\right) - \frac{3}{2} \ln \frac{16a^3}{v_w} \right) \equiv n_d kT f(\phi, a). \qquad [20] \end{aligned}$$

In this spirit the various choices for μ_d^0 correspond to the following volumes for the displacement of the center of mass of the fixed droplet.

Eq. [13], $V_{c.o.m.} = v_l$ (= molecular volume of the medium)

Safran and Turkevich (10), $V_{c.o.m.} = v_d$.

Eq. [15], $V_{c.o.m.} = v_d \exp(-18.25) = 1.2 \times 10^{-8}\, v_d$

Eq. [16], $V_{c.o.m.} = 0.134\, v_d n^{-3/2}$.

GIBBS ENERGY OF THE MICROEMULSION

The Gibbs energy of a microemulsion can be expressed more clearly by substituting the following expressions for Δp, V_d, and A in Eqs. [4] and [11]:

$$\Delta p = \frac{2\sigma}{a} - \frac{2c}{a^2} \qquad [21]$$

$$V_d = n_d v_d = \frac{4\pi}{3} a^3 n_d \qquad [22]$$

$$A = 4\pi a^2 n_d. \qquad [23]$$

Equation [21] for the excess pressure, Δp, inside a spherical droplet with radius a can be derived as follows. Consider an increase in the droplet radius with a length, da; then the work done by the pressure must be equal to the increase in interfacial free energy, or

$$\Delta p \cdot 4\pi a^2 da = d(4\pi a^2 \sigma) = 8\pi a\sigma da + 4\pi a^2 d\sigma$$

$$= 8\pi a\sigma da + 4\pi a^2 \left(\frac{\partial \sigma}{\partial(2/a)}\right)_{T,\lambda_i} d\left(\frac{2}{a}\right)$$

$$= (8\pi a\sigma - 8\pi c)da \qquad [24]$$

from which Eq. [21] follows directly. If the interfacial tension is curvature independent, so that $c = 0$, Eq. [21] simplifies to the classic Laplace equation, $\Delta p = 2\sigma/a$.

Substituting Eqs. [20] through [23] in Eqs. [4] and [11], we find

$$G^M = \sum n_i \lambda_i + n_d \frac{4\pi a^2}{3}\left[\sigma + \frac{2c}{a} + \frac{3kT}{4\pi a^2} f(\phi, a)\right] \qquad [25]$$

and

$$(dG^M)_{T,p} = \sum \lambda_i dn_i + \frac{4}{3}\pi a^2 \times \left[\sigma + \frac{2c}{a} + \frac{3kT}{4\pi a^2} f(\phi, a)\right] dn_d + n_d kT \times \frac{\partial f(\phi, a)}{\partial \phi} d\phi + n_d kT \frac{\partial f(\phi, a)}{\partial a} da. \qquad [26]$$

In order to prevent any misunderstanding, we stress that n_d, ϕ, a, and all n_i's are not independent of each other. A microemulsion, being a single phase, has only $q - 1$ degrees of freedom at constant T and p, if it is formed from q components plus, of course, the freedom involved in choosing its size. Therefore three of the variables in Eq. [26] depend on the others as will be shown in detail in the next section.

INTERNAL EQUILIBRIUM

In a microemulsion containing water, Nasa, NaCl, oil, and co (=alcohol), water, Nasa, and NaCl form the aqueous "phase," oil and co the oil "phase." Nasa and co are positively adsorbed and NaCl and oil are negatively adsorbed, *when we choose the Gibbs dividing surface such that water is not adsorbed* ($\Gamma_w = 0$). We choose from here on a W/O emulsion, but our treatment can also be applied to an O/W emulsion, although there the hard sphere approximation is less satisfactory due to the "softness" of the repulsion between electric double layers.

The area of the interface, A, between droplets and continuous medium is nearly fixed because most of the ionic surfactant is in the interface and saturation adsorption is reached for a wide range of concentrations (below the CMC) of the surfactant in the bulk of the droplets, as shown in the first paper of this series (20). Saturation adsorption implies that Γ_i does not depend on the concentration of i, although it may and often does depend on other parameters. Γ_{sa}, the amount of the ionic surfactant adsorbed per unit area, in particular

does depend somewhat on c(co), c(salt), and probably on the particle size. For A we may write

$$A = \frac{n_{sa} - n_{sa,d}}{\Gamma_{sa}} = 4\pi a^2 n_d, \qquad [27]$$

where $n_{sa,d}$ is the amount of surfactant (Nasa) in the droplets, and $n_{sa} - n_{sa,d}$ is the amount of surfactant adsorbed. Because in most cases of interest $n_{sa,d} \ll n_{sa}$, changes in $n_{sa,d}$ hardly affect A, but they may entail large changes in σ. The volume of the droplets is given by

$$V_d = n_w \bar{V}_w + (n_{Cl} - A\Gamma_{Cl})\bar{V}_{NaCl} + (n_{sa} - A\Gamma_{sa})\bar{V}_{Nasa} = \tfrac{4}{3}\pi a^3 n_d, \qquad [28]$$

where $\bar{V}_i$ is the molar volume of component i.

To keep the equations as simple as possible, we have neglected the solubility of the cosurfactant in the droplets and that of water, Nasa, and NaCl in the oil region.

With A and V_d given, a and n_d are simply found

$$a = \frac{3V_d}{A} = \frac{3\left\{n_w \bar{V}_w + \left(n_{Cl} - \dfrac{(n_{sa} - n_{sa,d})}{\Gamma_{sa}}\Gamma_{Cl}\right)\bar{V}_{NaCl} + n_{sa,d}\bar{V}_{Nasa}\right\}\Gamma_{sa}}{(n_{sa} - n_{sa,d})} \qquad [29]$$

and

$$n_d = \frac{A^3}{36\pi V_d^2} = \frac{(n_{sa} - n_{sa,d})^3 \Gamma_{sa}^{-3}}{36\pi\left\{n_w \bar{V}_w + \left(n_{Cl} - \dfrac{(n_{sa} - n_{sa,d})}{\Gamma_{sa}}\Gamma_{Cl}\right)\bar{V}_{NaCl} + n_{sa,d}\bar{V}_{Nasa}\right\}^2}. \qquad [30]$$

Whereas A, V_d, and a relate to the particle as bounded by the Gibbs dividing surface for $\Gamma_w = 0$, ϕ relates to the hard sphere volume, which should also include the mutually impenetrable parts of the adsorbed surfactant and cosurfactant molecules. We propose to include in the hard sphere drop volume, V_{hs}, all water, salt and surfactant and the adsorbed cosurfactant. This gives ϕ the value

$$\phi = \frac{V_{hs}}{V^M} = \frac{n_w \bar{V}_w + n_{sa}\bar{V}_{Nasa} + n_{Cl}\bar{V}_{NaCl} + A\Gamma_{co}\bar{V}_{co}}{V^M}$$

$$= \frac{n_w \bar{V}_w + n_{sa}\bar{V}_{Nasa} + n_{Cl}\bar{V}_{NaCl} + \dfrac{(n_{sa} - n_{sa,d})}{\Gamma_{sa}}\Gamma_{co}\bar{V}_{co}}{\sum\limits_{\text{all } i} n_i \bar{V}_i}. \qquad [31]$$

An alternative assumption, making the hard sphere radius larger than a by a constant length (e.g., $x + y$; see Eqs. [35] and [36]), leads to results very similar to those of Eq. [31].

As Eqs. [27] through [31] show, the detailed composition of a microemulsion expressed in A, V_d, a, n_d, and ϕ depends on the amounts of all components, n_i, and in addition on one further variable, for which we have chosen $n_{sa,d}$, the amount of surfactant dissolved in the droplets. For a microemulsion at equilibrium G^M is minimal; thus dG^M (Eq. [26]) = 0. This condition fixes the value of $n_{sa,d}$ and thus at equilibrium $n_{sa,d}$ itself is a function of all n_i's. The parameters $\bar{V}_i$ and Γ_i occurring in Eqs. [27] through [31] can be taken as known constants since the emulsion is in the region of saturation adsorption.

We now apply the equilibrium condition, $dG^M = 0$, to a microemulsion of a given composition (all $dn_i = 0$) and derive

$$\sigma + \frac{2c}{a} + \frac{3kT}{4\pi a^2} f(\phi, a) = -\frac{3n_d kT}{4\pi a^2} \times \left\{\frac{\partial f(\phi, a)}{\partial \phi}\left(\frac{\partial \phi}{\partial n_d}\right)_{n_i} + \frac{\partial f(\phi, a)}{\partial a}\left(\frac{\partial a}{\partial n_d}\right)_{n_i}\right\}$$

$$= -\frac{3n_d kT}{4\pi a^2}\left\{\frac{\partial f(\phi,a)}{\partial\phi}\left(\frac{\partial\phi/\partial n_{sa,d}}{\partial n_d/\partial n_{sa,d}}\right)_{n_i} + \frac{\partial f(\phi,a)}{\partial a}\left(\frac{\partial a/\partial n_{sa,d}}{\partial n_d/\partial n_{sa,d}}\right)_{n_i}\right\}. \quad [32]$$

In the differentiations in Eq. [32] we neglect the change of Γ_{sa}, Γ_{Cl}, and Γ_{co} with particle size, which has only a very minor influence here, but later we shall use the change of Γ_{sa} (and the surface charge density) with size explicitly in calculating c from model considerations (see Eqs. [56], [70], and ff). Straightforward but tedious algebra then leads to

$$\sigma + \frac{2c}{a} + \frac{3kT}{4\pi a^2} f(\phi,a) = -\frac{3kT}{4\pi a^2(1+2x/a)} \times\left(\frac{y\phi g(\phi)}{a+3(x+y)} + \frac{3(a+3x)}{2a}\right), \quad [33]$$

where

$$g(\phi) = \partial f(\phi,a)/\partial\phi = (1+\phi+\phi^2-\phi^3)/\phi(1-\phi)^3 \quad [34]$$

$$x = \Gamma_{sa}\bar{V}_{Nasa} + \Gamma_{Cl}\bar{V}_{NaCl} \text{ and } y = \Gamma_{co}\bar{V}_{co} \quad [35]$$

and n_d has been eliminated by using $n_d = 3V_d/4\pi a^3$, $V^M\phi = V_{hs}$, and

$$\frac{V_d}{V_{hs}} = \frac{V_d}{V_d + A(x+y)} = \frac{a}{a+3(x+y)}. \quad [36]$$

$n_{sa,d}$ is not explicitly present in Eq. [33], but it is implicit in σ and c. If σ and c are known as functions of the radius a and of the concentrations of co and sa ($c_{sa} = n_{sa,d}/V_d$), Eq. [33] can be used in a few successive approximations, starting, e.g., at c_{sa} = 0.5 CMC to find σ, c, c_{sa}, $n_{sa,d}$ and then a, n_d, and ϕ. The whole exercise leads only to a slight refinement of the values of a, n_d, and ϕ, as found from the equations [29] through [31] if $n_{sa,d}$ is simply taken equal to zero.

To give some impression about the quantities involved, we mention that x and y are both equal to about 4 Å (for NaDS, NaCl, and pentanol). With these values it is found that, as ϕ varies from 0.01 to 0.5 and a varies from 3 to 30 nm, $\sigma + 2c/a$ is always positive and varies between about 2 mN m^{-1} for the small radius to about 0.02 mN m^{-1} for the large radius.

COEXISTENCE OF A W/O MICROEMULSION WITH AN EXCESS AQUEOUS PHASE

When a droplet-type W/O microemulsion coexists with a noncolloidal aqueous phase, the composition of this phase might differ from that of the droplets. Therefore we calculate the chemical potentials, μ_i, of the aqueous components of the microemulsion and check under which conditions a simple noncolloidal phase exists with these same chemical potentials.

The μ_i's are found from $(\partial G^M/\partial n_i)_{n_{j\neq i},p,T}$ and of course the internal equilibrium condition [32] must be satisfied; i.e., $n_{sa,d}$ is now itself a function of all n_i's. We find then, using Eq. [26] for dG^M,

$$\mu_i = \left(\frac{\partial G^M}{\partial n_i}\right)_{n_{j\neq i},p,T} = \lambda_i + [1]\left(\frac{\partial n_d}{\partial n_i}\right)_{n_{j\neq i}} + [2]\left(\frac{\partial\phi}{\partial n_i}\right)_{n_{j\neq i}} + [3]\left(\frac{\partial a}{\partial n_i}\right)_{n_{j\neq i}} \quad [37]$$

with

$$[1] = \frac{4\pi a^2}{3}\left[\sigma + \frac{2c}{a} + \frac{3kT}{4\pi a^2} f(\phi,a)\right] = -[2]\left(\frac{\partial\phi}{\partial n_d}\right)_{\text{all } n_i} - [3]\left(\frac{\partial a}{\partial n_d}\right)_{\text{all } n_i} \quad [38]$$

and

$$[2] = n_d kT g(\phi) \quad \text{and} \quad [3] = -\frac{9n_d kT}{2a}. \quad [39]$$

With the use of

$$\left(\frac{\partial n_d}{\partial n_i}\right)_{n_{j\neq i}} = \left(\frac{\partial n_d}{\partial n_i}\right)_{n_{j\neq i},n_{sa,d}} + \left(\frac{\partial n_d}{\partial n_{sa,d}}\right)_{\text{all } n_i} \cdot \left(\frac{\partial n_{sa,d}}{\partial n_i}\right)_{n_{j\neq i}}, \quad [40]$$

analogous expressions for $(\partial\phi/\partial n_i)_{n_{j\neq i}}$ and $(\partial a/\partial n_i)_{n_{j\neq i}}$ and Eqs. [38] and [39], Eq. [37] can be transformed into

$$\mu_i = \lambda_i + n_d kTg(\phi)\left[\left(\frac{\partial\phi}{\partial n_i}\right)_{n_{j\neq i},n_{sa,d}} - \left(\frac{\partial\phi/\partial n_{sa,d}}{\partial n_d/\partial n_{sa,d}}\right)_{\text{all } n_i} \cdot \left(\frac{\partial n_d}{\partial n_i}\right)_{n_{j\neq i},n_{sa,d}}\right] - \frac{9n_d kT}{2a}\left[\left(\frac{\partial a}{\partial n_i}\right)_{n_{j\neq i},n_{sa,d}} - \left(\frac{\partial a/\partial n_{sa,d}}{\partial n_d/\partial n_{sa,d}}\right)_{\text{all } n_i} \times \left(\frac{\partial n_d}{\partial n_i}\right)_{n_{j\neq i},n_{sa,d}}\right]. \quad [41]$$

On evaluating the differential quotients, using again the Eqs. [28]–[31] and [34]–[36], one finds

$$\mu_i = \lambda_i + \bar{V}_i\left\{\frac{3kT}{4\pi a^3}\left[\frac{a\phi g(\phi)}{a+3(x+y)} \times \left(1-\phi+\frac{2y}{a+2x}\right) - \frac{3a}{2(a+2x)}\right]\right\} \quad [42]$$

which is exactly valid for i = w, NaCl, Nasa within the assumptions of our model. Defining

$$\chi \equiv \frac{3kT}{4\pi a^3}\left[\frac{a\phi g(\phi)}{a+3(x+y)} \times \left(1-\phi\frac{2y}{a+2x}\right) - \frac{3a}{2(a+2x)}\right] \quad [43]$$

we have

$$\mu_i = \lambda_i + \chi\bar{V}_i \quad \text{for w, NaCl, Nasa.} \quad [44]$$

λ_i is the chemical potential of component, i, in the droplet at a pressure $p + \Delta p$. At ambient pressure p the same composition would result in chemical potentials

$$\mu_i' = \lambda_i - \Delta p\bar{V}_i \quad [45]$$

and thus

$$\mu_i = \mu_i' + (\Delta p + \chi)\bar{V}_i. \quad [46]$$

In the transition from the solution corresponding to the μ_i''s to an equilibrium solution with the chemical potentials μ_i, all three chemical potentials change in the same direction. All three changes are positive or all three are negative according to Eq. [46]. Since this is not consistent with the Gibbs–Duhem relation the equilibrium solution must be identical to the droplet solution and thus we find as the *condition for external equilibrium*

$$\Delta p + \chi = 0 \quad [47]$$

or

$$\Delta p = \frac{2\sigma}{a} - \frac{2c}{a^2} = -\frac{3kT}{4\pi a^3}\left[\frac{a\phi g(\phi)}{a+3(x+y)} \times \left(1-\phi+\frac{2y}{a+2x}\right) - \frac{3a}{2(a+2x)}\right]. \quad [48]$$

By combining the two equilibrium conditions [33] and [48] we find σ and c separately for microemulsions in equilibrium with an aqueous phase.

$$\sigma = \frac{kT}{4\pi a^2}\left[-f(\phi,a) - \frac{a\phi g(\phi)}{a+3(x+y)} \times \left(1-\phi+\frac{3y}{a+2x}\right) - \frac{9x}{2(a+2x)}\right] \quad [49]$$

and

$$c = \frac{kT}{4\pi a}\left[-f(\phi,a) + \frac{a\phi g(\phi)}{2(a+3(x+y))} \times (1-\phi) - \frac{9}{4}\right]. \quad [50]$$

Equation [48] shows that in the two-phase equilibrium (W/O + W) the excess pressure, Δp, inside the droplets is positive at low ϕ, passes through zero at a volume fraction of about $\phi = 0.16$ (somewhat depending on the radius a and the values of x and y) and becomes negative for large volume fractions. In most cases Δp remains above -1 atm. For small ϕ the sign of Δp is determined by μ_d^0 (see Eq. [16]), and for large ϕ by the concentration dependence of G_{mix} (see Eq. [12]). Figure 2 gives curves of Δp against the reciprocal radius, $1/a$, for various values of ϕ, and a choice for x and y corresponding to SDS and pentanol as surfactant and cosurfactant respectively.

Of the two equilibrium conditions [49] and

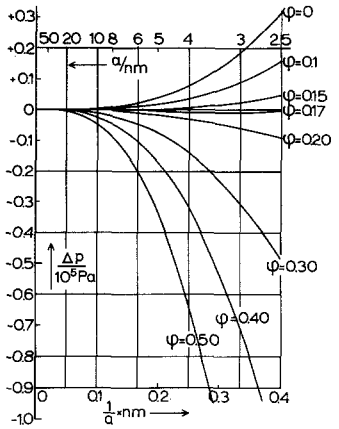

FIG. 2. Excess pressure, Δp, in the droplets against the reciprocal radius, $1/a$, for a W/O microemulsion, coexisting with an aqueous phase according to Eq. [48]. a = droplet radius; ϕ = volume fraction of droplets; $x = \Gamma_{sa}\bar{V}_{Nasa} + \Gamma_{Cl}\bar{V}_{NaCl} = 4$ Å; $y = \Gamma_{co}\bar{V}_{co} = 4$ Å.

[50] the equation for σ will be automatically satisfied by adjustment of the surfactant concentration $c_{sa} = n_{sa,d}/V_d$, while saturation adsorption is maintained (see Ref. (20)). Figure 3 shows that σ remains low (<1 mN m^{-1}) in practical circumstances.

Equation [50] for the bending stress coefficient, c, then determines the values of a and ϕ in the W/O + W equilibrium when the area A is given by the amount of surfactant and the drop volume V_d can adjust by expulsion or taking up of equilibrium liquid. c is a function of the curvature, $2/a$, and of the composition of droplets and dispersion medium, but not of ϕ. The rhs of Eq. [50] is a function of a and ϕ but with V_d variable and A constant, ϕ itself is a function of a. Thus Eq. [50] determines the equilibrium radius, a.

Figure 4 shows that c, as given by Eq. [50], must have values of the order of 10^{-12} N in order to allow the existence of Winsor II equilibria (or $\sim -10^{-12}$ N for Winsor I equilibria).

We therefore need to understand how c depends on a and other parameters.

MODEL OF THE INTERFACIAL REGION

In order to obtain the low interfacial tension essential for the stability of a microemulsion the adsorptions of surfactant and cosurfactant must both be in the saturation region (20). The hydrocarbon tails on the oil side are rather closely packed (about 25 Å^2 per group). On dissociation they form an electric double layer on the water side with a thickness proportional to the inverse square root of the electrolyte concentration.

The crowding of the tails tends to bend the interface around the water (concave at the water side). The electric free energy of the double layer tends to bend the interface around the oil, because that brings the counterions further apart and lowers the potentials at constant surface charge density. The balance of these

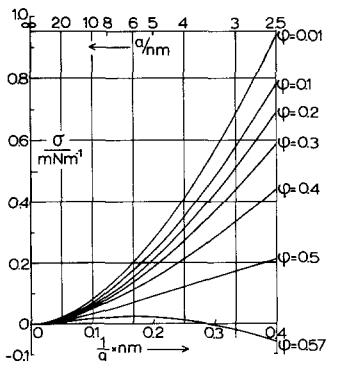

FIG. 3. Interfacial tension, σ, between droplets and medium in a W/O + W equilibrium according to Eq. [49]. Conditions as in Fig. 2.

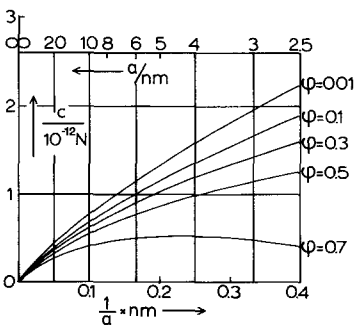

FIG. 4. Interfacial bending stress coefficient, c, according to Eq. [50] between droplets and medium in a W/O + W equilibrium. Conditions as in Fig. 2.

two tendencies determines the sign and the value of the preferred radius of curvature.

In Fig. 5 the interfacial tension, σ, and the bending stress coefficient, c, are plotted against the inverse radius, $1/a$. At the right $1/a$ is positive and the interface is curved around the water (W/O emulsions). Negative values of a are associated with curving around the oil (O/W type). The electric double layer makes a large contribution to σ at high W/O curvature and a weak contribution at the O/W side. For the tails the reverse is true. The combination of the two effects leads to an interfacial tension curve with a minimum for positive a if the tail effect is preponderant, but a minimum for negative a if the double layer wins.

The bending stress coefficient, c, has a positive slope against $1/a$. The interface has no tendency to change curvature when $c = 0$ (σ = minimal). The corresponding radius is called *natural radius, a**. In microemulsions $|a| < |a^*|$ since G(mix) (Eq. [12]) then decreases, due to the increase in the number of droplets, and allows some stress to remain in the interface.

These simple considerations allow a qualitative understanding of the transition O/W to W/O microemulsions and vice versa.

An increase in the electrolyte concentration lowers the potentials in the double layer (at constant surface charge density). It weakens the bending effect of the double layer and shifts σ, c, and $1/a^*$ to the right and this promotes W/O microemulsions.

An increase in the cosurfactant concentration increases the surface pressure of the tails, even at constant packing, strengthens the bending effect of the tails, and thus also promotes W/O structures.

Incidentally, an increase in the amount of surfactant only creates more interface, but does not affect the bending tendency directly.

We have used the Gibbs dividing surface for which $\Gamma_W = 0$ to define the radius, a. The charge layer (sulfate groups in SDS) will be close to the surface for which $\Gamma_W = 0$. On bending of the interface the adsorption remains saturated, because the activities of sa and co are high. But, since the ionic headgroups are not closely packed, but the tails nearly are, the surface of constant packing presumably is some way up the tails (close to the end of the pentanol chain?). We will therefore assume that the surface charge is located at a radius a and constant packing at radius $a + \xi$, with ξ = a few angstroms. This implies that the surface charge density changes with bending, being higher in W/O and lower in O/W situations.

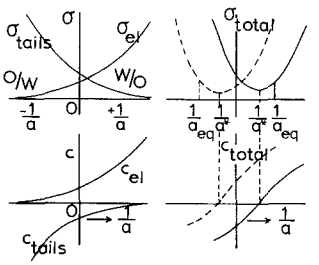

FIG. 5. Schematic curves for σ and c against $1/a$. In the figures on the left the contributions of the hydrocarbon tails and of the electric double layer are shown separately. At the right the drawn curves correspond to a large effect of the tails and a small effect of the double layer, resulting in a W/O emulsion with a *natural radius, a**, and a smaller equilibrium radius, a_{eq}. The dotted lines correspond to an O/W emulsion. The radius is counted positive when the center is at the water side, negative when it is at the oil side.

CONTRIBUTION OF THE ELECTRIC DOUBLE LAYER TO THE BENDING STRESS COEFFICIENT, c

The electrical contribution to the bending stress coefficient c_{el} is found from

$$c_{el} = \frac{dF_{el}(a, \sigma_{CH})}{d(2/a)}, \qquad [51]$$

where F_{el}, the electrical free energy per unit area of the double layer, is given by

$$F_{el} = \int_0^{\sigma_{CH}} \psi'_{surf}(a, \sigma'_{CH}) d\sigma'_{CH}. \qquad [52]$$

Here σ_{CH} is the surface charge density, assumed to be homogeneously smeared out, and ψ_{surf} is the potential at the surface.

Finding the relation between the surface charge density and the surface potential is difficult, because this involves solution of the Poisson–Boltzmann equation for high potentials and spherical symmetry, conditions for which no closed solution exists. Various authors have used numerical solutions or approximate expansions in a series. Loeb *et al.* (21) have made extensive numerical computations and they have given an empirical two-term series in $1/a$ for double layers *outside* a sphere. Levine and Robinson (22) solved the problem for low potentials *inside* a sphere and discussed approximate solutions for high potentials. Stokes (23) gave expansions in powers of $1/a$ for F_{el}, σ_{CH}, and ψ_{surf} *outside* a sphere. Mitchell and Ninham (8, 1983) developed equations very similar to those of Stokes and applied these to ionic micelles. Huh (9, 1983) used the results of Levine and Robinson, but not quite correctly. In the present paper we adapt the Stokes method to the double layer *inside* a sphere and take the above-mentioned shift parameter ξ into account. We have refrained from introducing further refinements such as incomplete dissociation and the presence of a Stern layer. This is probably not a bad approximation for charge densities normally observed in microemulsions.

The Poisson–Boltzmann equation for spherical symmetry and mono-monovalent electrolyte can be written as

$$\frac{d^2\Psi}{d(\kappa r)^2}+\frac{2}{(\kappa r)}\frac{d\Psi}{d(\kappa r)}=\sinh\Psi, \qquad [53]$$

where

$$\Psi=\frac{e\psi}{kT} \qquad [54]$$

and

$$\kappa^2=\frac{2e^2n_{el}}{\epsilon_r\epsilon_0 kT} \qquad [55]$$

where e is the elementary charge, n_{el} is the number of molecules of electrolyte per unit volume, ϵ_r is the dielectric constant of the aqueous medium, and ϵ_0 is the permittivity of the vacuum. ψ is the potential at a distance r from the center of the sphere and is zero at a location (not in the droplet) where the concentrations of cations and anions are both equal to n_{el}.

The surface charge density σ_{CH} is equal to

$$\Gamma_{sa}F=\sigma_{CH}=\epsilon_r\epsilon_0(d\psi/dr)_{r=a}. \qquad [56]$$

For low potentials ($\Psi \ll 1$)$\sinh\Psi \to \Psi$ and the solution of Eq. [53] can be given in closed form (22, 6),

$$\Psi=\Psi_a\frac{a\sinh\kappa r}{r\sinh\kappa a}=\frac{\sigma_{CH}a^2\sinh\kappa r}{\epsilon_r\epsilon_0 r(\kappa a\cosh\kappa a-\sinh\kappa a)}. \qquad [57]$$

This equation, although not directly applicable to W/O microemulsions, is often useful for checking the low potential limit of complicated expressions for high potentials.

Stokes (23) remarked that the relation between surface potential and surface charge density can be obtained without solving the Poisson–Boltzmann equation completely. Following his approach we define

$$H(\Psi,\kappa r)=\frac{d\Psi}{d(\kappa r)} \qquad [58]$$

and substituting H in Eq. [53] we find that H must satisfy

$$H\left(\frac{\partial H}{\partial\Psi}\right)_{\kappa r}+\left(\frac{\partial H}{\partial(\kappa r)}\right)_{\Psi}+\frac{2H}{\kappa r}-\sinh\Psi=0 \qquad [59]$$

with boundary conditions

$$H(r=a)=\frac{e}{kT}\frac{\sigma_{CH}}{\epsilon_r\epsilon_0\kappa} \text{ and } H(r=0)=0. \qquad [60]$$

Assume now that for large κr, H can be written as

$$H(\Psi,\kappa r)=\sum_{i=0}^{n}C_i(\Psi)/(\kappa r)^i. \qquad [61]$$

Substituting the series [61] into Eq. [59] and requiring that the coefficients for each term, $(\kappa r)^{-i}$, be zero lead to

$$C_0\frac{dC_0}{d\Psi}=\sinh\Psi;\ C_0\frac{dC_1}{d\Psi}+C_1\frac{dC_0}{d\Psi}+2C_0=0;$$

$$C_0\frac{dC_2}{d\Psi}+C_1\frac{dC_1}{d\Psi}+C_2\frac{dC_0}{d\Psi}+C_1=0;\ \text{etc.} \qquad [62]$$

Solving the first of these equations yields

$$C_0 = 2\sqrt{\sinh^2(\Psi/2) - \sinh^2(\Psi_m/2)} \cong 2\sinh(\Psi/2), \quad [63]$$

where Ψ_m is the dimensionless potential in the middle of the sphere. With C_0 known, the second equation [62] can be solved for C_1 and then C_2 follows from the third equation. All expressions for C_i contain contributions of Ψ_m, necessary to make C_i = zero at the center of the sphere. If these contributions are neglected by putting $\Psi_m = 0$, the following result is obtained:

$$\frac{d\Psi}{d(\kappa r)} \equiv H(\kappa r, \Psi) = 2\sinh\frac{\Psi}{2} - \frac{4\tanh(\Psi/4)}{\kappa r} - \frac{4(\tanh^2(\Psi/4) - 2\ln\cosh(\Psi/4))}{(\kappa r)^2\sinh(\Psi/2)} \cdots . \quad [64]$$

A fourth term, proportional to $(\kappa r)^{-3}$, may be easily added, but shall be omitted here. The series [64] is identical to the one given by Stokes, except for a change of sign of the terms with uneven powers of κr, as expected since the signs of the curvature are different in the two cases.

A conservative estimate of the errors introduced by taking $\Psi_m = 0$ has been made by calculating Ψ_m from Eq. [57] (certainly an overestimate) and comparing the values of C_i with and without the Ψ_m terms. The errors decrease rapidly with increasing r, are larger for C_1 than for C_0 and for C_2, just reach 2% in C_1 for $\kappa r = 4$ and stay under 0.5% in C_1 (much lower in C_0 and C_2) for $\kappa r = 5$. We conclude that Eq. [64] is a good approximation for $\kappa r = 5$, acceptable for $\kappa r = 4$ and possibly for $\kappa r = 3$, but unsatisfactory below $\kappa r = 3$. This limits the applicability for Eq. [64] to droplets of $a \geqslant 4$ nm at 0.1 M NaCl and to $a \geqslant 2.5$ nm at 0.3 M NaCl.

For the integration of Eq. [52] it is advantageous to have Ψ_{surf} as a function of H rather than H as a function of Ψ_{surf}. We therefore invert the series [64] and specialize the result to $r = a$.

$$\Psi_a = \frac{e\psi_a}{kT} = 2\ln(p+q) + \frac{1}{\kappa a}\frac{4(q-1)}{pq} + \frac{1}{(\kappa a)^2}\left\{\frac{4(q-1)^2(2q+1)}{p^3q^3} - \frac{4\ln((q+1)/2)}{pq}\right\}, \quad [65]$$

where

$$p = \frac{H_a}{2} = \sqrt{q^2-1} \quad \text{and}$$

$$q = \sqrt{p^2+1} = \sqrt{\frac{H_a^2}{4}+1}. \quad [66]$$

Now the integral [52] can be calculated, resulting in

$$F_{el} = \left(\frac{kT}{e}\right)^2 \epsilon_r\epsilon_0\kappa\left\{4(p\ln(p+q) - q + 1) + \frac{8}{\kappa a}\ln\left(\frac{q+1}{2}\right) + \frac{4}{(\kappa a)^2}\left(\frac{(q+2)(q-1)}{q(q+1)} + \int_{z=2/(1+q)}^{z=1}\frac{\ln z\,dz}{(1-z)}\right)\cdots\right\}. \quad [67]$$

The integral in Eq. [67] can be expressed in two power series

$$\int_x^1 \frac{\ln z\,dz}{1-z} = -\frac{\pi^2}{6} + \ln x\ln(1-x) + \sum_{i=1}^{\infty}\frac{x^i}{i^2} \quad [68a]$$

and

$$\int_x^1 \frac{\ln z\,dz}{1-z} = -\sum_{i=1}^{\infty}\frac{(1-x)^i}{i^2} \quad [68b]$$

of which the first converges more rapidly for $x < 0.5$ or $H_a > 5.66$ and the second for $x > 0.5$ or $H_a < 5.66$. For water at room temperature, H_a (see Eq. [60]) is about 5.66 for $\sigma_{CH} = e/90$ Å^2 and an electrolyte concentration of 0.3 M.

Now c_{el} can be found simply by differentiating F_{el} with respect to $2/a$ (see Eq. [51]).

The result is

$$c_{el} = \frac{dF_{el}(a, \sigma_{CH})}{d(2/a)} = \left(\frac{\partial F_{el}}{\partial(2/a)}\right)_{\sigma_{CH}} + \left(\frac{\partial F_{el}}{\partial \sigma_{CH}}\right)_a \times \frac{d\sigma_{CH}}{d(2/a)} = \frac{1}{2}\frac{\partial F_{el}}{\partial(1/a)} + \frac{1}{2}\psi_{surf}(a, \sigma_{CH}) \cdot \frac{d\sigma_{CH}}{d(1/a)}. \quad [69]$$

Using Eqs. [60] and [65]–[67] and taking into account the shift ξ between the radii of the surface charge, a, and the surface of constant packing, $a + \xi$, by putting

$$\sigma_{CH} = \sigma_{CH}(\text{flat}, a \to \infty) \cdot (a + \xi)^2/a^2 \quad [70]$$

and thus

$$p = p(\text{flat})(a + \xi)^2/a^2 \quad \text{and}$$

$$q = \sqrt{p^2(\text{flat})(1 + \xi/a)^4 + 1} \quad [71]$$

Eq. [69] can be worked out, leading to

$$c_{el} = 4\left(\frac{kT}{e}\right)^2 \epsilon_r \epsilon_0 \left\{\ln\left(\frac{q+1}{2}\right) + \kappa\xi p \ln(p+q) + \frac{1}{\kappa a}\left(\frac{(q+2)(q-1)}{q(q+1)} + \int_{2/(1+q)}^{1} \frac{\ln z\, dz}{(1-z)} + \frac{4\kappa\xi(q-1)}{q} + \kappa^2\xi^2\left(p \ln(p+q) + \frac{2p^2}{q}\right)\right)\right\}. \quad [72]$$

In Eq. [72] all p's and q's stand for p(flat) and q(flat). The numerical values of the various terms in Eq. [72] are such that the $\kappa\xi$ and $\kappa^2\xi^2$ terms are larger, in certain cases much larger, than the $\kappa\xi$ free terms even for ξ as small as 2 Å when the NaCl concentration is 0.1 M or larger.

CONTRIBUTION OF THE LIPOPHILIC TAILS TO THE BENDING STRESS

As mentioned before the mutual repulsion among the close-packed hydrocarbon tails will tend to curve the interface around the aqueous side. Mukherjee *et al.* (7) and Huh (9) worked out theories for the free energy contribution of lipophilic tails anchored at a curved interface. Unfortunately these theories cannot be easily adapted to fit the situation of (nearly) close packing where the surface pressure is regulated by the bulk concentrations of surfactant and cosurfactant. We therefore preferred to work with an empirical equation

$$c_{tails} = -D \exp(-l/a), \quad [73]$$

where l is a length of the order of the hydrocarbon chain length, and D is a positive constant that may depend on the concentration of the cosurfactant. Equation [73] shows the required (see Fig. 5) negative value for $a \to \infty$, a positive slope with the reciprocal radius, $1/a$, and it tends to zero for high W/O curvature (large $1/a$).

The bending stress coefficient c_{tot} is then simply found by addition of the contributions of the tails and the double layer:

$$c_{tot} = c_{el} + c_{tails}. \quad [74]$$

NUMERICAL ILLUSTRATIONS

In Fig. 4 and Eq. [50], c has been given as a function of a and ϕ for a two-phase Winsor II (W/O + W) equilibrium. Equations [72] through [74] allow the calculation of c as a function of a. Combination of Eqs. [50] and [74] gives the relation between ϕ and a for this equilibrium. Unfortunately c in Eq. [74] contains several parameters. However, if the theoretical calculations are combined with experimental data only one of these parameters can be chosen freely within fairly narrow limits as will be shown now.

p and q in Eq. [72] follow via Eqs. [66], [60], and [56] from the amount of surfactant adsorbed per unit area and this is or can be determined from interfacial tension measurements on a macroscopic interface (20). κ is known from the electrolyte concentration and Eq. [55]. For an oil phase containing 81% cyclohexane and 19% (w/w) pentanol (final concentrations) and aqueous phases containing 0.099 and 0.297 M NaCl respectively the saturation adsorption of SDS, Γ_{sa}, has been measured (20). Values for a few other NaCl concentrations have been estimated by interpo-

lation or a short extrapolation. The results are given in Table I.

The Value of the Parameter ξ

Now we make a choice for ξ (see Eq. [70]) for which a first guess is half the length of the pentanol molecule, say 0.4 nm. This choice fixes c_{el} as a function of a. From experiments (24) with microemulsions of aqueous NaCl solutions, cyclohexane, SDS, and pentanol we know that at 19% (w/w) pentanol in cyclohexane the *optimal salinity* (salt concentration where O/W switches to W/O) is at about 0.15 M NaCl. For this salt concentration c(total) must be zero for $a \to \infty$ and thus D (Eq. [73]) $= c_{el}$ (0.15 M, $a \to \infty$), which fixes D. At the same pentanol concentration, but 0.3 M NaCl, the water droplet radius at a volume fraction $\phi = 0.05$ (chosen so low in order to minimize the influence of adsorption on salt and cosurfactant concentrations) is about 6 nm, which fixes the value of l. Consequently we have one combination of ξ, D, and l that fits experimental data. For each choice of ξ such a combination is found. The higher the value of ξ, the higher the slope of c against $1/a$, and the smaller the influence of the volume fraction, ϕ, on the equilibrium radius a_{eq}. This is desirable since experimentally hardly any influence of ϕ on a_{eq} is found (24). But there is only a narrow margin for ξ. At $\xi = 0.5$ nm the desired radius of 6 nm at 0.3 M NaCl and an optimal salinity of 0.15 M cannot be obtained even at $l = 0$. At the other extreme $\xi = 0$ does not lead to a stable radius of 6 nm and $\xi = 0.1$ nm still results in too great a change of a with ϕ ($a = 3.97^5$ nm at $\phi = 0.01$ to $a = 10.15$ nm at $\phi = 0.5$). In between these extremes acceptable results are obtaining for ξ varying from 0.2 to 0.4 nm. Table II and Fig. 6 give a few illustrative results. In Fig. 7 the influence of ϕ on a_{eq} is shown for a few selected cases. In the middle region ($\phi = 0.1$ to 0.4) the lines have a rather small slope, in particular for $\xi = 0.3$ (not drawn) and 0.4 nm. Negative adsorption of NaCl in the double layer leads to an increase in the effective NaCl concentration at higher values of ϕ and compensates, or even overcompensates, the direct influence of ϕ on a (see Ref. (24)).

Influence of the Electrolyte Concentration

In Fig. 8 values for c (Eq. [74]) have been plotted showing how equilibrium droplet radii increase with lowering of the electrolyte concentration. The curve for 0.1 M NaCl does not intersect the $c(a, \phi)$ curves for two-phase equilibrium at positive values of a, indicating that at this concentration O/W emulsions are formed. The theoretical transition from O/W to W/O is chosen to occur at about 0.15 M NaCl.

Influence of the Concentration of the Cosurfactant

Although in the region of interest surfactant and cosurfactant are adsorbed to saturation,

TABLE I

Combinations of 1–1 Electrolyte Concentrations, Surfactant Adsorptions, and Values of κ^{-1}, and p Derived therefrom, to be Used in Eq. [72] and in Figs. 6 through 11

Electrolyte concentration (m)	0.1	0.15	0.16	0.18	0.20	0.25	0.298	0.30	0.40
κ^{-1} (Eq. [55] (nm)	0.9608	0.7845	0.7595[5]	0.7161	0.6794	0.6076	0.5566	0.5547	0.4804
Γ_{sa} (SDS) (μmole m^{-2})	1.56[5]	1.66	1.67[5]	1.70[5]	1.73	1.78	1.82	1.82	1.89
$\sigma_{sa} = \Gamma_{sa} \times F$ (C m^{-2})	0.1510	0.1602	0.1616	0.1645	0.1669	0.1717	0.1756	0.1756	0.1824
H ($r = a$) (Eq. [60])	8.145	7.055	6.891	6.613	6.366	5.859	5.487	5.468	4.918
p (Eq. [66]) $= H/2$	4.0725	3.527	3.4455	3.3065	3.183	2.929	2.743[5]	2.734	2.459

Note. The values of Γ_{sa} for 0.1 and 0.3 M (actually 0.298 M) are based on measurements (20); the values for other concentrations have been estimated by linear interpolation of Γ_{sa} vs log(conc) or by a short extrapolation. The ratio of pentanol to cyclohexane in the oil phase is 19/81 (w/w). The temperature is 25°C. The electrolyte is NaCl.

TABLE II

Combinations of ξ (Eq. [70]), l, and D (Eq. [73]), all Leading to an Optimal Salinity of about 0.15 M NaCl for 19% (w/w) Pentanol in Cyclohexane, with the Resulting Droplet Radii, a, for 0.3 M NaCl, as a Function of the Volume Fraction, ϕ, in W/O + W Two-Phase Equilibria

Volume fraction, ϕ	0.5	0.3	0.1	0.05	0.01	Conclusions
$\xi = 0$; $D = 1.55$; $l = 11.99$	24.94	22.35	19.49[5]	18.06	14.26	No stable radius for $a = 6.0$
$\xi = 0.1$; $D = 3.17$[5]; $l = 3.061$	10.15	8.48	6.79	6.0	3.97[5]	Too much variation in a
$\xi = 0.2$; $D = 4.80$; $l = 1.544$	8.91	7.66	6.50	6.0	4.99[5]	All three acceptable ξ = 0.4; l = 0.3056 gives the smallest variation in a
$\xi = 0.3$; $D = 6.42$; $l = 0.7944$	8.41	7.36	6.40	6.0	5.21	
$\xi = 0.4$; $D = 8.04$[5]; $l = 0.3056$	8.10	7.19	6.35	6.0	5.31	
$\xi = 0.5$; $D = 9.67$; $l = 0$	8.70	7.84	7.06	6.73	6.07[5]	Even for $l = 0$ radius at $\phi = 0.05$ larger than 6.0.

Note. ξ, l, and a are in nanometers, D in 10^{-12} N. Where possible l has been chosen such that the radius for $\phi = 0.05$ is equal to 6.0 nm.

an increase in the concentration of cosurfactant leads to an increase in the surface pressure. This might be expected to promote bending of the interface around the water side and it could explain that more cosurfactant leads to Winsor II (W/O + W) equilibria with droplet size decreasing as c_{co} increases. However, the primary influence of the cosurfactant is found to be a small but significant decrease in Γ_{sa} with increasing c_{co} as determined in Ref. (20).

From the experimental relation between the optimal salinity and c_{co} (24) and the interpolated values of Γ_{sa} for these optimal salinities, $D = c_{el}$ ($a \rightarrow \infty$) can be found for each concentration of cosurfactant. Remarkably, D changes little with c_{co} at least for $\xi = 0.3$ and 0.4 nm. We further assume that the decay

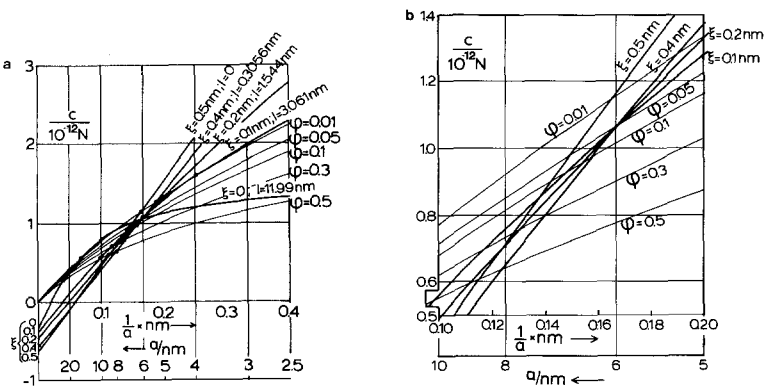

FIG. 6. (a) c vs $1/a$ lines for a few combinations of ξ, l, and D, as mentioned in Table II, all at 19% (w/w) pentanol/cyclohexane and 0.3 M NaCl, calculated with Eqs. [72]–[74]. Also c vs $1/a$ as given by the two-phase equilibrium condition, Eq. [50]. The points of intersection give the values of a_{eq}. (b) Enlargement of part of Fig. 6a.

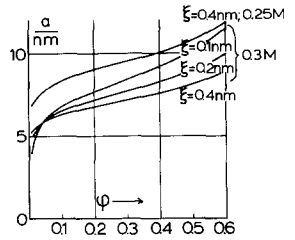

FIG. 7. Showing that for reasonable choices of ξ the equilibrium radius depends little on the volume fraction between $\phi = 0.05$ and 0.4, but somewhat more outside these limits.

length, l (see Eq. [73]), of the tail effect is independent of c_{co}. This gives enough information for calculating c_{tot} (Eq. [74]) for various cosurfactant concentrations. The effect of c_{co} on the dielectric constant of the aqueous medium is small, and since the influence of ϵ_r on c_{el} contains a great deal of internal compensations ($\epsilon_r \kappa p$ does not depend on ϵ_r) it has been neglected.

In Fig. 9 we show the effect of the cosurfactant concentration on the equilibrium radii and volume fractions. The data used for Γ_{sa} and the optimal salinities are collected in Table III.

Influence of the Concentration of the Ionic Surfactant

As mentioned earlier most of the ionic surfactant is adsorbed and Γ_{sa} is known from the Gibbs adsorption equation (20). Thus the amount of surfactant fixes the total droplet area A and with a known from the composition of the system, V_d and ϕ can be found from Eqs. [29] and [31], respectively.

In the one-phase region V_d is known from the composition and a adapts itself to Eq. [29].

Interfacial Tension between Coexisting Phases

The interfacial tension between the microemulsion and the equilibrium solution, γ_{MW}, differs from the interfacial tension of the droplets, σ, for two reasons. The interfacial tension is curvature dependent, and moreover, σ, as introduced in Eqs. [3] and [6], belongs to the chemical potentials, λ_i, whereas γ_{MW} is the interfacial tension at the chemical potentials μ_i, the difference being due to the free mobility of the drops in the final situation. Consequently γ_{MW} is related to σ by

$$\gamma_{MW}(a \to \infty, \mu_i) = \sigma(a, \lambda_i) + \int_a^{a\to\infty} \times \left(\frac{\partial\sigma}{\partial(2/a)}\right)_{\lambda_i} d\left(\frac{2}{a}\right) + \sum_i \int_{\lambda_i}^{\mu_i} \left(\frac{\partial\sigma}{\partial\mu_i}\right)_{a\to\infty} d\mu_i. \quad [75]$$

With the use of Eqs. [6], [7], and [44], Eq. [75] can be transformed into

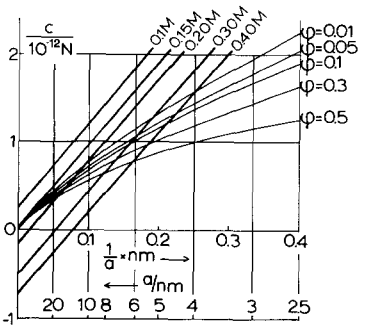

FIG. 8. Illustrating the influence of the NaCl concentration on equilibrium radii. With 19% pentanol the disappearance of the W/O + W boundary is found at about 0.15 M NaCl. ξ, l, and D are 0.3 nm, 0.7944 nm, and 6.42 $\times 10^{-12}$ N, respectively; cf. Table II.

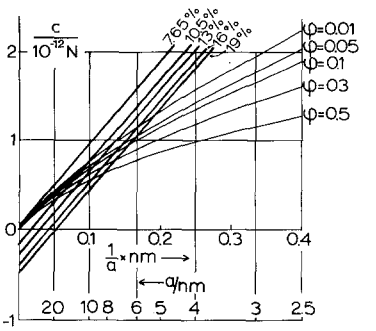

FIG. 9. Influence of the cosurfactant concentration in the oil medium (%, (w/w) pentanol/cyclohexane) on equilibrium combinations of radii, a, bending stress coefficients, c, and volume fractions, ϕ, in Winsor II equilibria. See Table III for further details.

TABLE III

Data Used in Fig. 9 for the Demonstration of the Influence of the Cosurfactant Concentration via the Parameters Γ_{sa} and D on Winsor II Phase Equilibria

Initial concn. pentanol in cyclohexane, % (w/w)	1	5	8.6	9.25	10	11.5	14	17	20
Final concn pentanol, % (w/w)	0.55	4.11	7.65	8.25	9	10.5	13	16	19
Γ_{sa} (μmole m^{-2}) at 0.1 M NaCl	2.21[5]	1.752	1.663	1.653	1.643	1.625	1.60	1.58	1.56[5]
Γ_{sa} (μmole m^{-2}) at 0.3 M NaCl	2.4	2.0	1.915	1.905	1.895	1.877	1.855	1.835	1.82
p (at 0.3 M NaCl)			2.877	2.862	2.847	2.820	2.787	2.757	2.734
Initial concn pentanol in cyclohexane (%), w/w at 1% SDS/water			9.4	10	10.75	12.2	14.66	17.6	20.6
Optimal salinity (M NaCl)			0.30	0.283	0.268	0.240	0.205	0.172	0.15
Γ_{sa} at optimal salinity (μmole m^{-2})			1.915	1.892	1.869	1.826	1.767	1.706	1.66
κ^{-1} (nm) at optimal salinity			0.5547	0.5711	0.5869	0.6202	0.6710	0.7326	0.7845
p at optimal salinity			2.877	2.926	2.971	3.067	3.211	3.385	3.527
$D = c_{el}$ (optimal salinity $a \to \infty$) (10^{-12} N); $\xi = 0.3$ nm			6.356	6.360	6.359	6.365	6.377	6.403	6.422[a]
$D = c_{el}$ (optimal salinity $a \to \infty$), (10^{-12} N); $\xi = 0.4$ nm			8.045	8.044	8.036	8.030	8.026	8.038	8.046[a]

Note. Γ_{sa} for initial pentanol concentrations of 1, 5, and 20% at 0.30 M NaCl and of 1 and 20% at 0.1 M NaCl are based on measurements reported in Ref. (20). The other values are obtained by linear interpolation against log(concn NaCl) and against $1/\sqrt{c_{co}}$. The values of the optimal salinities are taken from Ref. (24). Further conditions are 0.3 M NaCl, $\kappa^{-1} = 0.5547$ nm, $l = 0.7944$ nm for $\xi = 0.3$ nm, and $l = 0.3056$ nm at $\xi = 0.4$ nm.

[a] The small differences between these values and those of Table II are due to rounding off in Table II.

$$\gamma_{MW} = \sigma + 2\int_a^{a\to\infty} cd\left(\frac{1}{a}\right) - (\Gamma_{sa}\bar{V}_{Nasa} + \Gamma_{Cl}\bar{V}_{NaCl})\chi + (\Gamma_o\bar{V}_o + \Gamma_{co}\bar{V}_{co})\Pi, \quad [76]$$

where Π is the osmotic pressure caused by the droplets. In the Gibbs formalism, as we use it, the interface has no volume and thus (see Eq. [35])

$$\Gamma_{sa}\bar{V}_{Nasa} + \Gamma_{Cl}\bar{V}_{NaCl} = -(\Gamma_o\bar{V}_o + \Gamma_{co}\bar{V}_{co}) = x. \quad [77]$$

According to Eq. [47], $\chi = -\Delta p$ and Δp is given in Eq. [48]. In the Percus–Yevick–Carnahan–Starling approximation the osmotic pressure Π can be written (see Ref. (6, 1978)) as

$$\Pi = RT\frac{\phi}{V_{HS}}\frac{(1+\phi+\phi^2-\phi^3)}{(1-\phi)^3} = \frac{3kT}{4\pi a^2}\frac{\phi^2 g(\phi)}{a+3(x+y)}, \quad [78]$$

where Eqs. [34] and [36] have been applied. Using Eq. [49] for σ and [72] through [74] for c, we can transform γ_{MW} from Eq. [76] into Eq. [79]:

$$\gamma_{MW} = \frac{kT}{4\pi a^2}\left[-\ln\phi + \frac{3}{2}\ln\frac{16a^3}{v_w} - \frac{\phi(7-3\phi-\phi^2)}{(1-\phi)^2} - \frac{3\phi(x+y)(1+\phi+\phi^2-\phi^3)}{(a+3(x+y))(1-\phi)^3}\right]$$
$$- 8\left(\frac{kT}{e}\right)^2 \epsilon_r\epsilon_0\left[\frac{1}{a}\left\{\ln\left(\frac{q+1}{2}\right) + \kappa\xi p\ln(p+q)\right\} + \frac{1}{2\kappa a^2}\left\{\frac{(q+2)(q-1)}{q(q+1)}\right.\right.$$
$$\left.\left. + \int_{2/(1+q)}^{1}\frac{\ln z\,dz}{(1-z)} + \frac{4\kappa\xi(q-1)}{q} + \kappa^2\xi^2\left(p\ln(p+q) + \frac{2p^2}{q}\right)\right\} + \frac{2D}{l}\left\{1-\exp\left(-\frac{l}{a}\right)\right\}\right]. \quad [79]$$

If combinations of a and σ in two-phase equilibria are known, e.g., from figures such as Figs. 6–9, interfacial tensions, γ_{MW}, can be calculated. Figures 10 and 11 give a few examples showing that calculated γ_{MW}'s are generally low (<0.2 mN m^{-1}) and that they drop steeply when "optimal salinity" or "optimal cosurfactant concentration" is approached. Note the logarithmic scale for γ_{MW}. The same figures show how the droplet radius increases with decreasing γ_{MW}, i.e., with decreasing salt and/or cosurfactant concentration. Figure 11 also shows that good agreement with experiments can be obtained. For the radii the agreement is nearly perfect. The calculated values of γ_{MW} are slightly too high, in all cases less than a factor of 2. Here one should remember that the only data used in the calculations are a few values of the surfactant adsorption, Γ_{sa}, a single value for the particle radius (a = 6 nm) at 19% pentanol and 0.3 M NaCl, and the combinations of salt and pentanol concentrations where the radii go to infinity. From these few data all equilibrium radii, a, and interfacial tensions γ_{MW} were calculated.

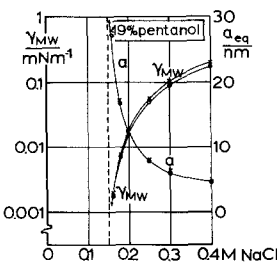

FIG. 10. Calculated interfacial tension, γ_{MW}, between microemulsion and equilibrium aqueous phase against the NaCl concentration. Also particle radii, a_{eq}. Note the logarithmic scale for γ_{MW} and the linear scale for a_{eq}. Pentanol/cyclohexane 19% (w/w); ϕ = 0.05; (×) ξ = 0.4 nm; (○) ξ = 0.3 nm.

The agreement between theory and experiments might be improved by further refinements, such as incomplete dissociation (or penetration of counterions "behind" the charged surface groups) and a more negative value of μ^θ (Eq. [16]) because water is rather incompressible.

It should be realized that for large droplet size (say a > 20 nm) two effects that have been neglected here become more and more important. For large droplets c is always rather small. This implies that small forces suffice to change the radius of curvature. Consequently fluctuations become relatively more important, leading to a wider size distribution, deviations from the spherical shape, and, ultimately, to the formation of bicontinuous systems.

Second, interdroplet attractions, whether of the long-range van der Waals type, or due to short-range attractions between the tails of the surfactants on two droplets, become more important for large droplets, thus requiring a correction on hard sphere behavior. This may lead to phase separation and is then the basis for the formation of the third phase in Winsor III equilibria.

So far we have concentrated our attention on microemulsions in two-phase equilibria. We will briefly discuss now what happens when the composition of a mixture does not

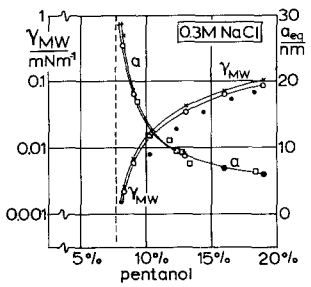

FIG. 11. Calculated interfacial tension, γ_{MW}, and particle radius, a_{eq}, against pentanol concentration in the oil medium. NaCl, 0.3 M; $\phi = 0.05$; (×) $\xi = 0.4$ nm; (○) $\xi = 0.3$ nm; (●) experimental interfacial tension and (□) experimental radii taken from Ref. (24).

correspond to such an emulsion. If the ratio of brine to surfactant is too large, the radius a is too large for the given salt and cosurfactant concentration, c is too small, and Δp is larger than the Δp in the two-phase equilibrium. Consequently brine is pressed out of the droplets forming as much of the equilibrium phase as needed to bring a and σ to the required equilibrium values. On the other hand, if the ratio of brine to surfactant is too small, smaller droplets are formed, c is higher as given by the c vs $2/a$ lines (Eqs. [72]–[74]), the interface becomes stiffer, and the droplets are more spherical and more isodisperse. Δp is smaller than the value of Eq. [48] and the droplets have a tendency to suck up more brine if that becomes available. The microemulsion formed is in the one-phase region. A proof for the increased stiffness of the interfaces might perhaps be found in dynamic measurements.

CONCLUSIONS

The thermodynamic theory of phase equilibria of microemulsions, in particular Winsor II (W/O + W) equilibria, presented here, explains the influence of the concentrations of electrolyte, cosurfactant, and ionic surfactant on the droplet radius, the interfacial tension, and the volume fraction.

Specific aspects of the theory are

1. *Surfactant* and *cosurfactant* are both adsorbed to saturation, and together drive the interfacial tension down to nearly zero. Since most of the surfactant is at the droplet interface and its amount per unit area, Γ_{sa}, can be measured (20) the amount of surfactant present determines the interfacial area A, and with the radius, a, following from the theory it also determines the volume fraction, ϕ.

2. The *curvature dependence* of the interfacial tension expressed in a bending stress coefficient, c, is essential.

3. The *interfacial tension, σ, of the droplets* and c are found as functions of a and ϕ without involving a specific model for the interface. A choice has been made for the standard chemical potential, μ_d^θ, of the droplets (Eq. [16]) in the free energy of mixing.

4. A *model calculation* for c as a function of a has been given and, together with the relation $c(a, \phi)$ mentioned in point 3, this allows the calculation of a and γ_{MW}, the interfacial tension between the macroscopic phases.

5. The contribution of the *electric double layer* to the bending stress has been calculated. Although the surface charge density increases slightly with increasing salt content the main effect of the salt is a decrease in the double-layer thickness resulting in a smaller tendency of the interface to bend around the oil side. It is necessary to take into account that the surface charge density is increased by a stronger curvature around the water side, due to a small distance, $\xi \sim 0.2$–0.4 nm, between the surface of charge and the surface of constant packing density.

6. The *cosurfactant* has a twofold influence on c. It promotes curvature around the oil side by the mutual repulsion between the hydrocarbon tails, but, somewhat surprisingly, this effect hardly depends on the cosurfactant concentration. The main effect of the concentration is due to a slight but significant decrease in the adsorption of the ionic surfactant at increased cosurfactant concentration.

7. The influence of the *volume fraction, ϕ,* on a and γ_{MW} at constant concentrations of salt and cosurfactant is small but not negligible. However, higher ϕ entails more negative

adsorption of salt and positive adsorption of cosurfactant which complicates the direct effect of ϕ. Comparison with experiments will be presented in a later publication. In this paper we have compared the theory with experiments at only one, fairly low, volume fraction, $\phi = 0.05$.

8. *Measured radii* over a fairly wide range of cosurfactant concentrations fit the theory quite nicely, if one radius at one concentration and a set of combinations of salt and cosurfactant concentrations where the radii go to infinity are used to fit the parameters in the theory.

9. Calculated *interfacial tensions,* γ_{MW}, are slightly (up to a factor of 1.8) higher than measured values, but follow the same trend (over a factor of 50) as the experiments. This is the more gratifying since no parameters other than those used for the calculation of the radii have been introduced.

ACKNOWLEDGMENTS

We are grateful to Mrs. Marina Uit de Bulten for the preparation of the typescript and to Mr. Theo Schroote for drawing the figures. The investigation was supported by the Netherlands Foundation of Chemical Research (SON) with financial aid from the Netherlands Organisation for the Advancement of Pure Research (ZWO).

REFERENCES

1. Winsor, P. A., *Trans. Faraday Soc.* **44,** 376 (1948).
2. Robbins, M. L., *in* "Micellization, Solubilization and Microemulsions" (K. L. Mittal, Ed.), Vol. 2, p. 713. Plenum, New York, 1977.
3. Reiss, H., *J. Colloid Interface Sci.* **53,** 61 (1975); *Adv. Colloid Interface Sci.* **7,** 1 (1977).
4. Ruckenstein, E., and Chi, J. C., *J. Chem. Soc. Faraday Trans. 2* **71,** 1690 (1975); Ruckenstein, E., *Chem. Phys. Lett.* **57,** 517 (1978); *J. Colloid Interface Sci.* **66,** 369 (1978); *Soc. Pet. Eng. J,* 593 (1981); *Chem. Phys. Lett.* **98,** 573 (1983); **118,** 435 (1985).
5. Wagner, C., *Colloid Polym. Sci.* **254,** 400 (1976).
6. Overbeek, J. Th. G., *Faraday Discuss. Chem. Soc.* **65,** 7 (1978); Overbeek, J. Th. G., de Bruyn, P. L., and Verhoeckx, G. J. *in* "Surfactants" (Th. F. Tadros, Ed.), p. 111. Academic Press, New York, 1984; Overbeek, J. Th. G., *in* "Debye Symposium, Proc. Kon. Ned. Akad. Wetenschap. B," Vol. 89, p. 61. 1986.
7. Miller, C. A., and Neogi, P., *AIChE J.* **26,** 212 (1980); Mukherjee, S., Miller, C. A., and Fort, T. Jr., *J. Colloid Interface Sci.* **91,** 223 (1983); Miller, C. A., *J. Dispersion Sci. Technol.* **6,** 159 (1985).
8. Mitchell, D. J., and Ninham, B. W., *J. Chem. Soc. Faraday Trans. 2* **77,** 601 (1981); *J. Phys. Chem.* **87,** 2996 (1983).
9. Huh, C., *Soc. Pet. Eng. J.* **23,** 829 (1983); *J. Colloid Interface Sci.* **97,** 201 (1984).
10. Safran, S. A., and Turkevich, L. A., *Phys. Rev. Lett.* **50,** 1930 (1983); Safran, S. A., *J. Chem. Phys.* **78,** 2073 (1983).
11. Talmon, Y., and Prager, S., *J. Chem. Phys.* **69,** 2984 (1978).
12. de Gennes, P. G., and Taupin, C., *J. Phys. Chem.* **86,** 2294 (1982).
13. Bowcott, J. E., and Schulman, J. H., *Z. Elektrochem.* **59,** 283 (1955); Schulman, J. H., and Montagne, J. B., *Ann. N. Y. Acad. Sci.* **92,** 366 (1961); Stoeckenius, W., Schulman, J. H., and Prince, L. M., *Kolloid-Z.* **169,** 170 (1960).
14. Agterof, W. G. M., van Someren, J. A. J., and Vrij, A., *Chem. Phys. Lett.* **43,** 363 (1976); Caljé, A. A., Agterof, W. G. M., and Vrij, A., *in* "Micellization, Solubilization and Microemulsions" (K. L. Mittal, Ed.), Vol. 2, p. 779. Plenum, New York, 1977; Vrij, A., Nieuwenhuis, E. A., Fijnaut, H. M., and Agterof, W. G. M., *Faraday Discuss Chem. Soc.* **65,** 101 (1978).
15. Murphy, C. L., Ph.D. thesis, University of Minnesota, 1966.
16. Melrose, J. C., *Ind. Eng. Chem.* **60,** 53 (1968).
17. "The Collected Works of J. Willard Gibbs," Vol. I, p. 225. Yale Univ. Press, New Haven, reprinted 1948; Originally, *Trans. Conn. Acad. Arts. Sci.* **3,** 343 (1878).
18. Percus, J. K., and Yevick, G. J., *Phys. Rev.* **110,** 1 (1958).
19. Carnahan, N. F., and Starling, K. E., *J. Chem. Phys.* **51,** 635 (1969); **53,** 600 (1970).
20. Verhoeckx, G. J., de Bruyn, P. L., and Overbeek, J. Th. G., *J. Colloid Interface Sci.* **119,** 409 (1987).
21. Loeb, A. L., Overbeek, J. Th. G., and Wiersema, P. H., "The Electrical Double Layer around a Spherical Colloid Particle," pp. 37, 39, 46 ff. MIT Press, Cambridge, 1961.
22. Levine, S., and Robinson, K., *J. Phys. Chem.* **76,** 876 (1972).
23. Stokes, A. N., *J. Chem. Phys.* **65,** 261 (1976).
24. Verhoeckx, G. J., de Bruyn, P. L., and Overbeek, J. Th. G., to be published.